

## Supporting Information

### **Efficient and ultra-broadband Cr<sup>3+</sup>/Ni<sup>2+</sup> co-doped phosphors for light-emitting diodes with spectral output over NIR-I and NIR-II regions**

Qianyi Jia,<sup>a</sup> Leqi Yao,<sup>\*b</sup> Shijie Yu,<sup>a</sup> Shuxuan Gong,<sup>a</sup> Jianqing Jiang<sup>c</sup> and Qiyue Shao<sup>\*a</sup>

<sup>a</sup> School of Materials Science and Engineering, Jiangsu Key Laboratory for Advanced Metallic Materials, Southeast University, Nanjing 211189, P. R. China

E-mail: qiyueshao@seu.edu.cn

<sup>b</sup> Jiangsu Bree Optronics Co., Ltd., Nanjing 211103, P. R. China

E-mail: yaoleqi@163.com

<sup>c</sup> School of Mechanical and Electronic Engineering, Nanjing Forestry University, Nanjing 210037, P. R. China

**Table S1** Amounts of the reagents used for the phosphor synthesis.

	MgO (mol)	Ga <sub>2</sub> O <sub>3</sub> (mol)	MgF <sub>2</sub> (mol)	Cr <sub>2</sub> O <sub>3</sub> (mol)	NiO (mol)	
MGO	1.000	1.000	-	-	-	
MGOF	0.950	0.900	0.250	-	-	
MGOF:0.06Cr <sup>3+</sup> , yNi <sup>2+</sup>	y = 0	0.950	0.870	0.250	0.030	-
	y = 0.005	0.945	0.870	0.250	0.030	0.005
	y = 0.01	0.940	0.870	0.250	0.030	0.010
	y = 0.02	0.930	0.870	0.250	0.030	0.020
	y = 0.04	0.910	0.870	0.250	0.030	0.040
	y = 0.06	0.890	0.870	0.250	0.030	0.060
MGOF:xCr <sup>3+</sup> , 0.005Ni <sup>2+</sup>	x = 0	0.945	0.900	0.250	-	0.005
	x = 0.01	0.945	0.895	0.250	0.005	0.005
	x = 0.02	0.945	0.890	0.250	0.010	0.005
	x = 0.04	0.945	0.880	0.250	0.020	0.005
	x = 0.06	0.945	0.870	0.250	0.030	0.005
	x = 0.08	0.945	0.860	0.250	0.040	0.005

**Table S2** Refined crystallographic data for MGOF:0.06Cr<sup>3+</sup>, yNi<sup>2+</sup> (y = 0, 0.005, 0.01, 0.04).

	y = 0	y = 0.005	y = 0.01	y = 0.04
Space group			Cubic	
Symmetry			<i>Fd<math>\bar{3}m</math></i>	
a(Å)	8.1299	8.1107	8.1093	8.0984
$\alpha = \gamma(^{\circ})$			90.000	
Z			8	
V(Å <sup>3</sup> )	537.35	533.55	533.26	531.13
Ga/Cr/Ni/Mg-O length (Å)	1.9538	1.9567	1.9502	1.9560
$R_{wp}(\%)$	11.33	9.61	7.75	8.64
$R_p(\%)$	7.18	6.58	5.36	6.30
$\chi^2$	7.56	5.53	3.72	5.11

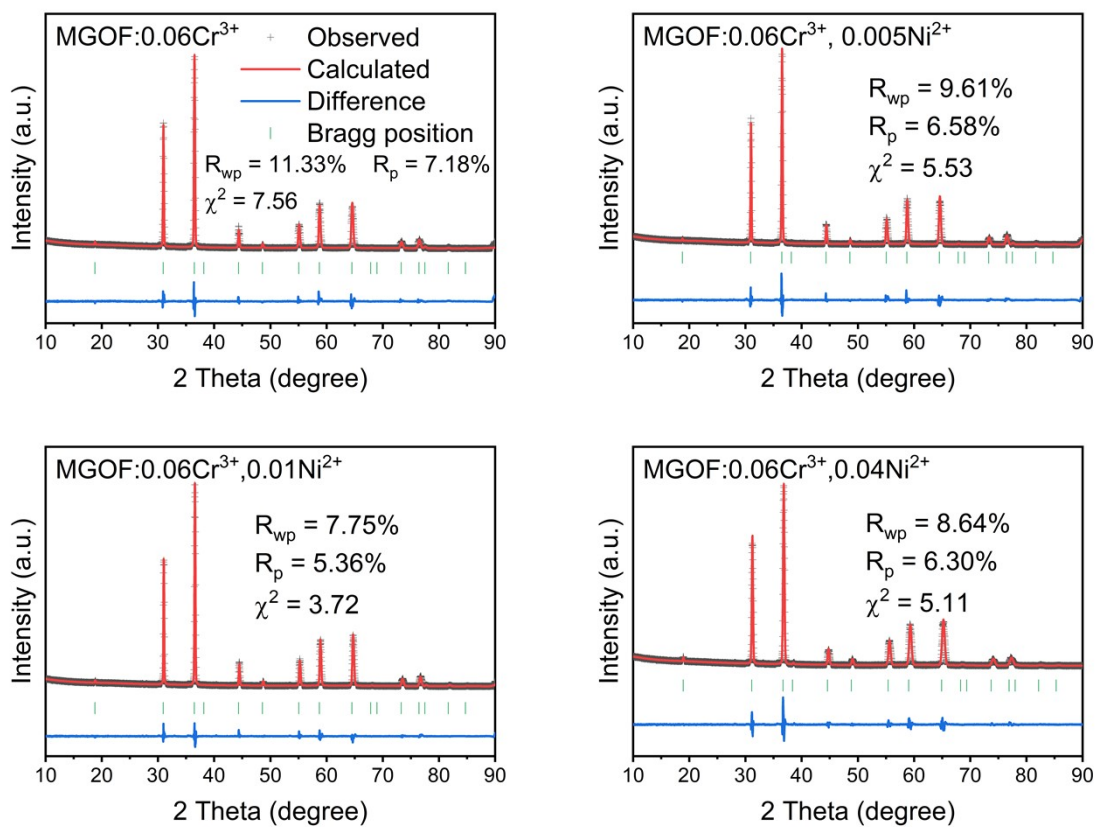


**Figure S1.** Rietveld refinements of XRD profiles for MGOF:0.06Cr<sup>3+</sup>, yNi<sup>2+</sup> (y = 0–0.04) samples.

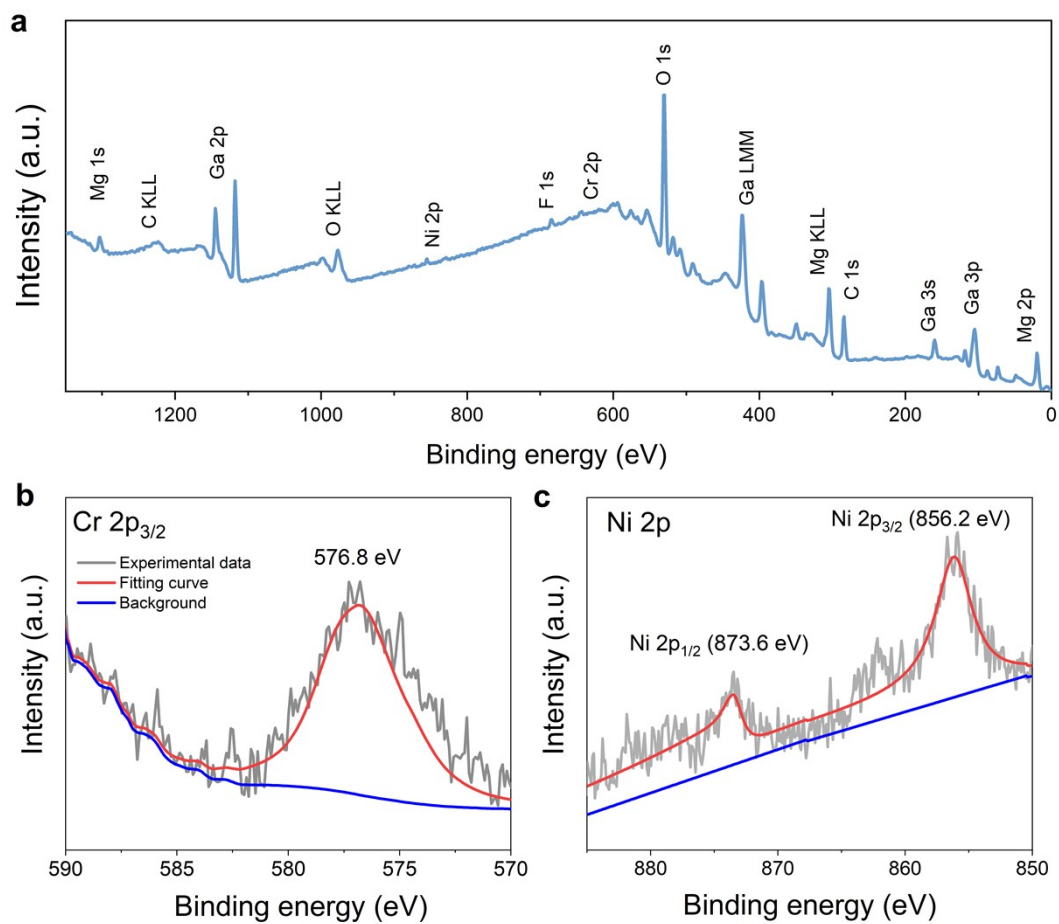


**Figure S2.** a) XPS survey scan, and b) Cr 2p<sub>3/2</sub> and c) Ni 2p high resolution XPS spectra of the MGOF:0.06Cr<sup>3+</sup>, 0.04Ni<sup>2+</sup> sample.

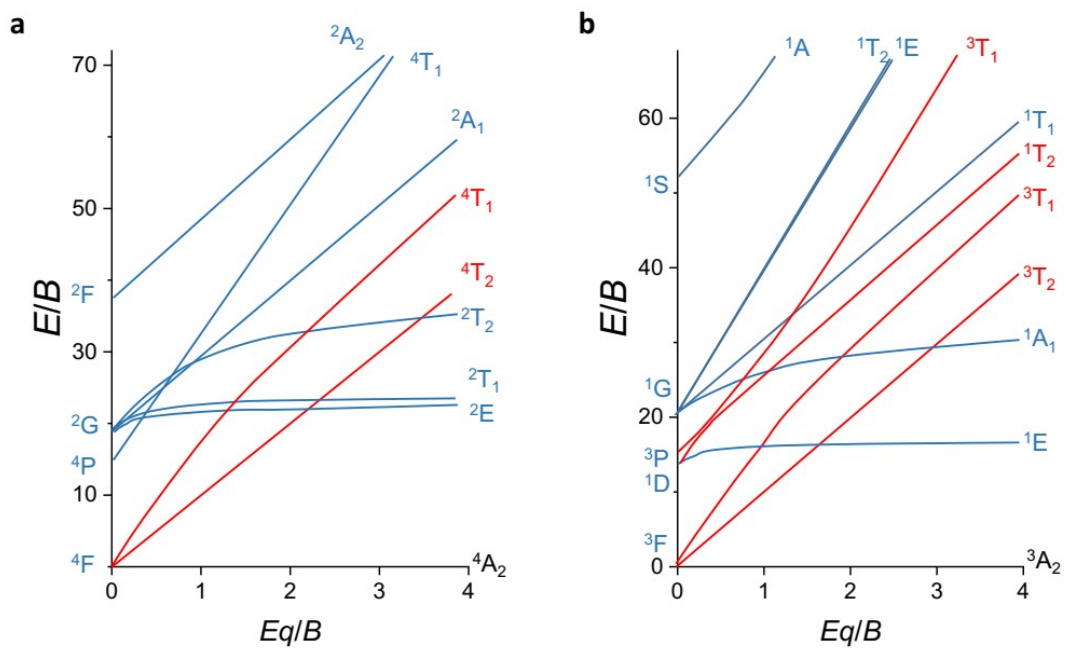


**Figure S3.** Tanabe–Sugano energy level diagrams of a)  $\text{Cr}^{3+}$  and b)  $\text{Ni}^{2+}$  ions in octahedral coordination.

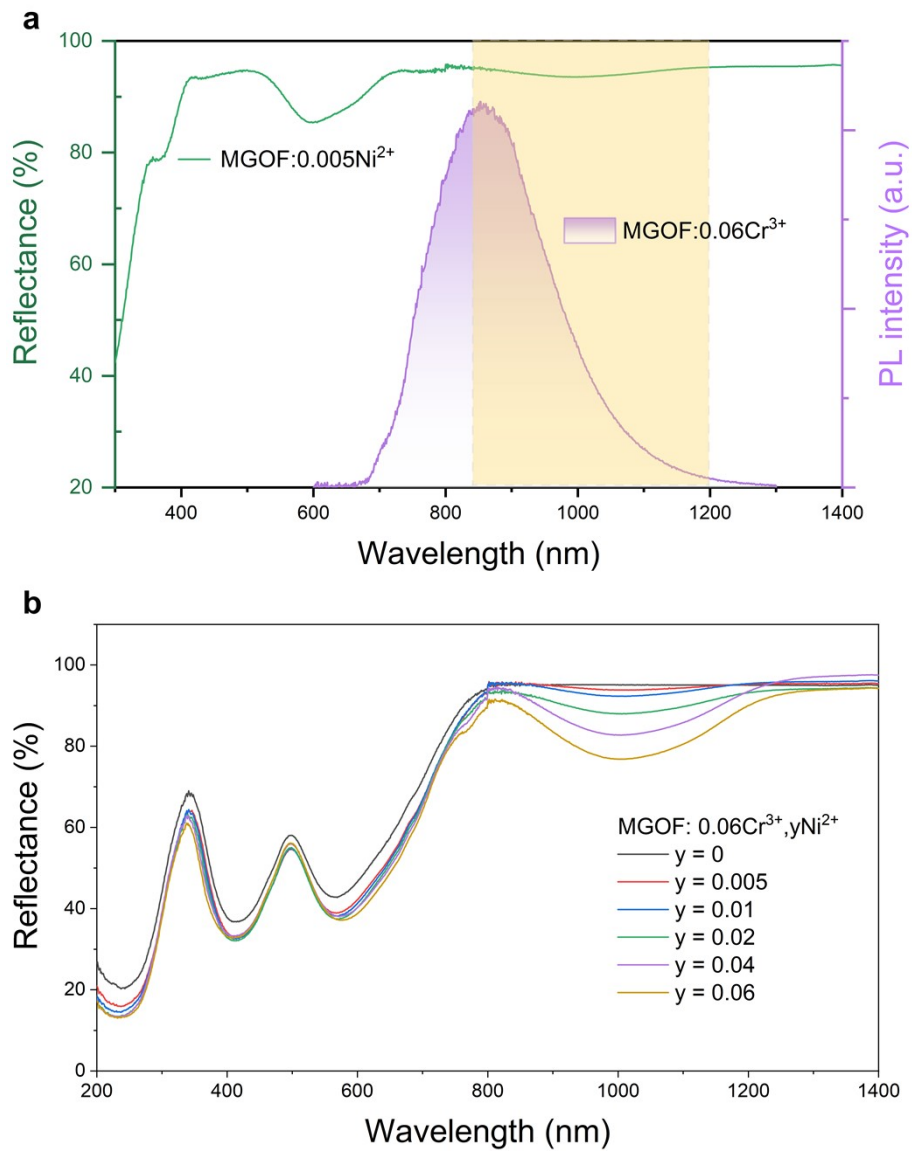


**Figure S4.** a) The diffuse reflection spectrum of the MgO:F:0.005Ni<sup>2+</sup> phosphor and the emission spectrum of the MgO:F:0.06Cr<sup>3+</sup> phosphor under 420 nm excitation; b) Diffuse reflection spectra of the MgO:F:0.06Cr<sup>3+</sup>,yNi<sup>2+</sup> ( $y = 0-0.06$ ) phosphors.

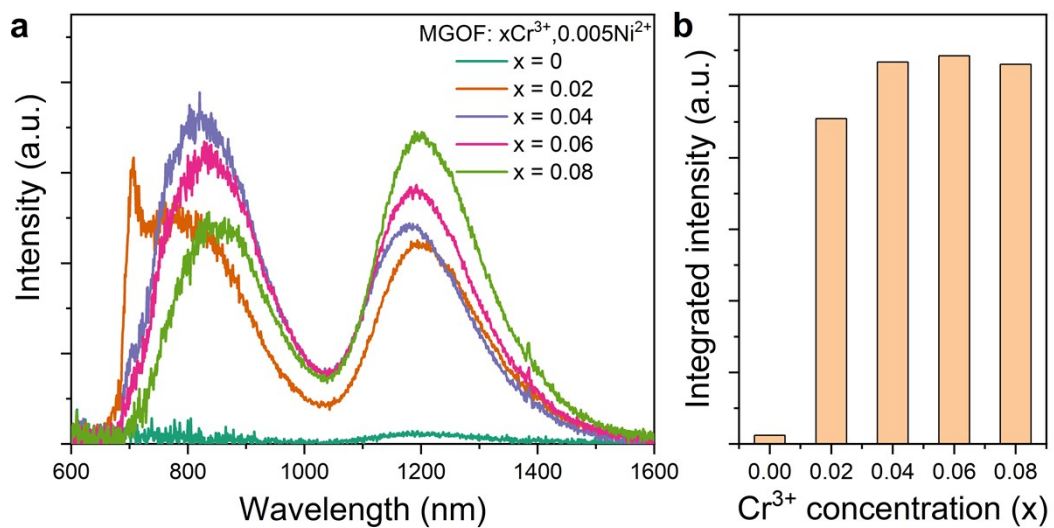


**Figure S5.** a) PL emission spectra and b) integrated intensities of MGOF: $x\text{Cr}^{3+}, 0.005\text{Ni}^{2+}$  phosphors with various  $x$  values under 420 nm excitation.



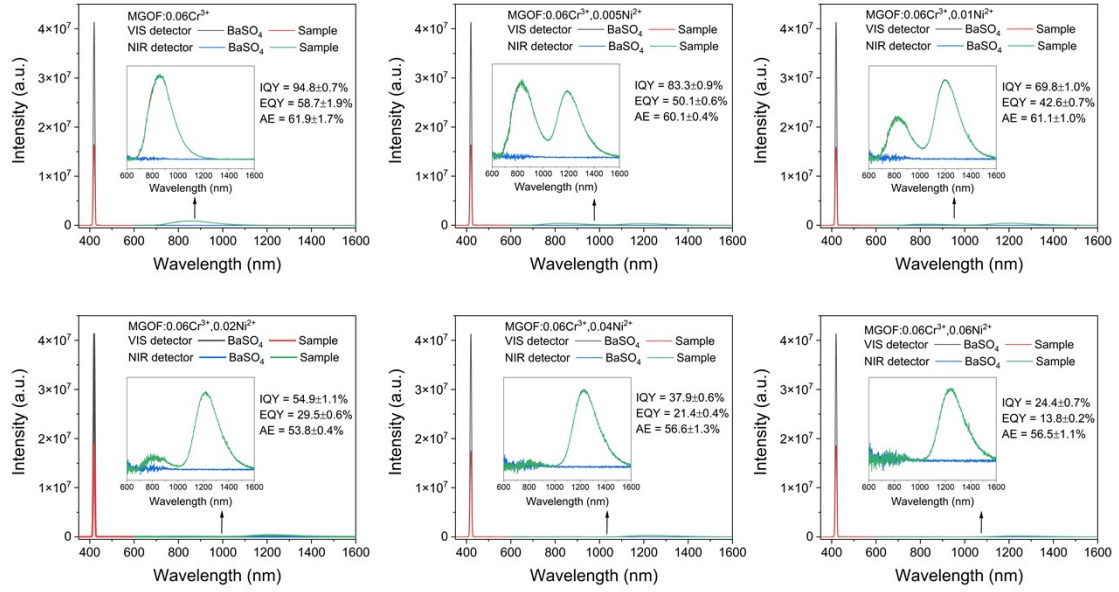


**Figure S6.** Quantum efficiency measuring spectra of MGOF:0.06Cr<sup>3+</sup>, yNi<sup>2+</sup> phosphors (y = 0, 0.005, 0.01, 0.02, 0.04 and 0.06).

The internal quantum efficiency (IQE), external quantum efficiency (EQE) and absorption efficiency (AE) are calculated using the following equations:

$$IQE = \frac{\int L_S - \int L_R}{\int E_R - \int E_S} \times 100\% \quad (S1)$$

$$EQE = \frac{\int L_S}{\int E_R} \times 100\% \quad (S2)$$

$$AE = \frac{\int E_R - \int E_S}{\int E_R} \quad (S3)$$

Where  $L_S$  and  $L_R$  are the luminescent spectra of the sample and reference (BaSO<sub>4</sub>), respectively.  $E_S$  and  $E_R$  are the excitation light spectra for the sample and reference, respectively. The FLS1000 spectrophotometer is equipped with two photodetectors, but both cannot respond accurately in a broad spectral range from the blue to NIR light. Therefore, the excitation spectra ( $E_S$  and  $E_R$ ) were measured by the visible (VIS) detector, while the luminescent spectra ( $L_S$  and  $L_R$ ) were measured by the NIR detector. The difference in sensitivity of the two detectors was carefully calibrated by successively measuring the luminescent spectra of the sample in the spectral range of 600–820 nm. Both VIS and NIR detectors can accurately respond in 600–820 nm. Accordingly, the luminescent spectrum  $L_S$  is calibrated by the following equation:

$$L_S = \left( \int_{820}^{650} L_{VIS} / \int_{820}^{650} L_{NIR} \right) \times L_{NIR} \quad (S4)$$

where  $L_{VIS}$  and  $L_{NIR}$  represent the luminescent spectrum of the sample recorded by the VIS and NIR detector, respectively. After calibration,  $L_S$ ,  $E_S$  and  $E_R$  can be obtained in the same response ability.

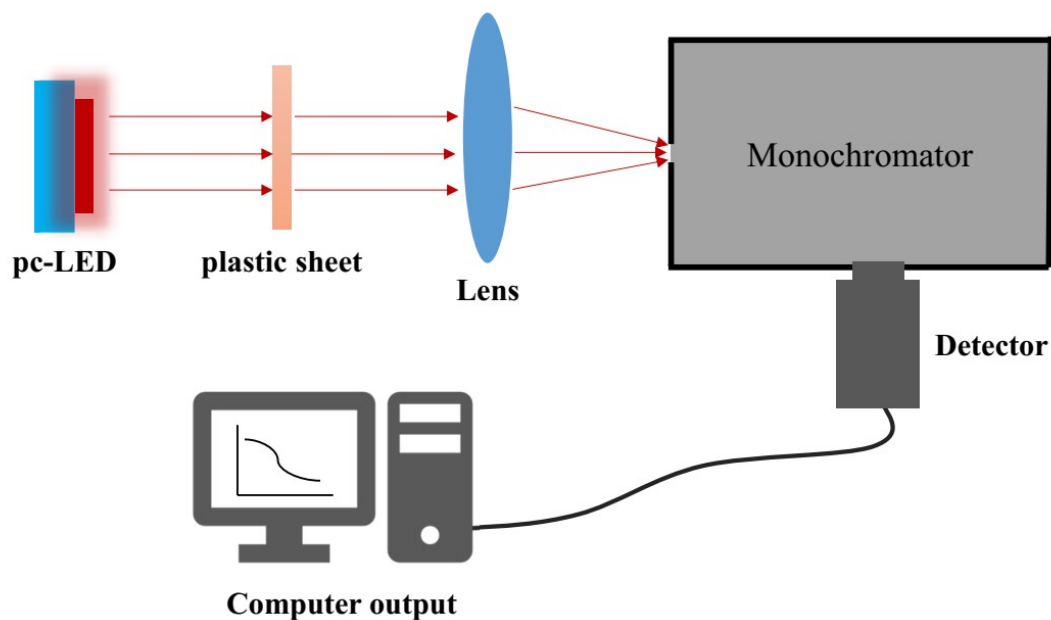


**Figure S7.** Schematic diagram of the testing system for the spectral absorption of plastic sheets (thickness  $\sim 3$  mm) in transmission mode. The testing system was set up on basis of the emission monochromator and the NIR detector (responsive wavelengths: 500–1600 nm) of the FLS1000 spectrometer. Using the fabricated pc-LED as the external light source, the spectral signals after penetrating the plastic sheets were collected and analyzed by the emission monochromator, and then recorded by the NIR detector.

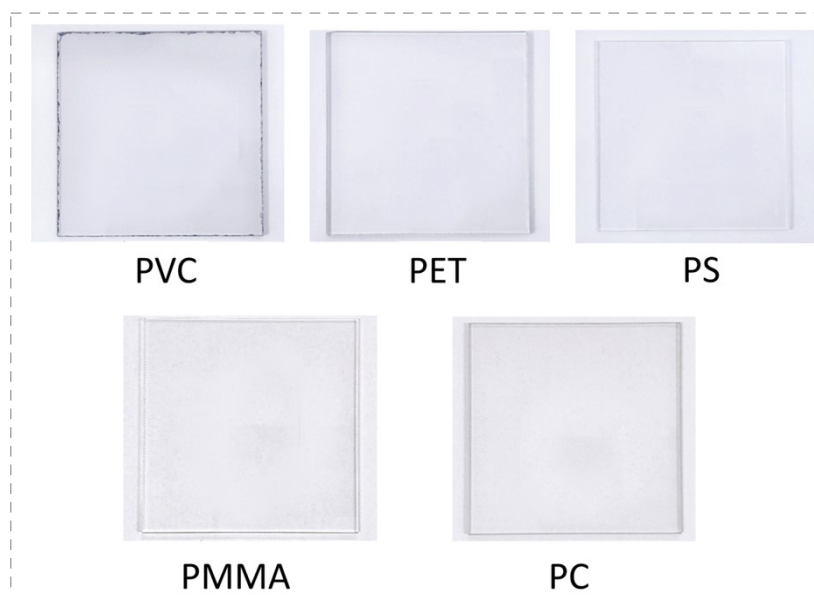


**Figure S8.** Photographs of plastic sheets including polyvinyl chloride (PVC), polyethylene terephthalate (PET), polystyrene (PS), polymethyl methacrylate (PMMA), and polycarbonate (PC).